Cyclic Tau-derived peptides for stabilization of microtubules

Hiroshi Inaba,[1,2]* Miyuu Nagata,[1] Kyeongmi Juliano Miyake,[1] Arif Md. Rashedul Kabir,[3] Akira Kakugo,[3,4] Kazuki Sada,[3,4] Kazunori Matsuura[1,2]*

[1]Department of Chemistry and Biotechnology, Graduate School of Engineering, Tottori University, Tottori 680-8552, Japan.

[2]Centre for Research on Green Sustainable Chemistry, Tottori University, Tottori 680-8552, Japan.

[3]Faculty of Science, Hokkaido University, Sapporo 060-0810, Japan.

[4]Graduate School of Chemical Sciences and Engineering, Hokkaido University, Sapporo 060-0810, Japan.

E-mails: hinaba@tottori-u.ac.jp, ma2ra-k@tottori-u.ac.jp

Running Head: Cyclic peptides for stabilization of microtubules

ABSTRACT

The cyclization of peptides is a valuable strategy for the development of binding motifs to target proteins with improved affinity. Microtubules (MTs) are important targets for therapeutics, and a variety of MT-targeted drugs and peptides have recently been developed. We have previously designed a Tau-derived peptide (**TP**) that binds to the interior of MTs. In the present study, the development of a cyclic **TP** (**TCP**) for enhanced binding to tubulin and the stabilization of MTs is described. The fluorescently labeled cyclic peptide containing three glycine linkers (**TCP3-TMR**) exhibited a remarkably enhanced binding affinity to tubulin. The cyclic peptide was also demonstrated to stabilize MTs by enhancing polymerization and reducing depolymerization. Moreover, MTs were effectively formed by the treatment of cyclic peptides in the presence of guanosine triphosphate (GTP), while the linear peptide showed no such effect. These findings indicate that **TCP** is a useful binding motif that can stabilize MTs and is valuable for various therapeutic and material applications.

Key Words: Microtubule / Peptide / Tau-derived peptide / Cyclic peptide

INTRODUCTION

Peptides are attractive binding motifs for targeting proteins with high selectivity and affinity. Protein-binding peptides can be utilized for various applications, such as the inhibition of protein-protein interactions, signaling, and cell adhesion [1–5]. Cyclic peptides have superior properties compared to their linear counterparts, including improved binding affinity, target selectivity, cellular uptake capability, and high proteolytic stability [6–10]. The higher binding affinity of cyclic peptides can be explained by the lower entropic loss upon binding to target proteins [11]. Linear peptides typically adopt disordered conformations in aqueous solutions and display defined conformations upon binding to target proteins. The restriction in conformational freedom upon binding leads to an entropic penalty, which affects the affinity for the target proteins. On the other hand, in the case of cyclic peptides, the conformational freedom is restricted in solution, and the entropic loss resulting from binding to the target proteins is minimized, leading to high affinity. Owing to their unique properties, cyclic peptides are valuable protein binding motifs for various applications, including therapeutics. For example, Suga et al. developed a screening library of cyclic peptides for the development of various drug candidates [9].

Microtubules (MTs) are cytoskeletal structures that are widely recognized as important therapeutic targets for the treatment of MT-related diseases, such as cancer and neurodegenerative disorders [12, 13]. MTs are hollow tube assemblies formed by the polymerization of tubulin dimers. The balance between the polymerization and depolymerization of MTs as well as the motility of motor proteins (e.g., kinesin and dynein) on MTs are critical in a number of cellular processes, such as cell division [14, 15]. Due to the importance of MTs, various MT-targeted drugs that disrupt their dynamics by binding to tubulin have been developed [12, 13]. Taxol (paclitaxel) is one of the most well-known anticancer agents. It stabilizes MTs by binding to their inside pocket, inducing tubulin polymerization and inhibiting depolymerization [16]. Since the Taxol binding pocket in

MTs is a unique target for the design of novel therapeutic molecules, a number of peptides that bind in this pocket of MTs have been developed [17–20]. The reported peptides bind to the Taxol binding pocket with moderate affinities to promote tubulin polymerization. Campiani et al. designed linear and cyclic peptides, which were shown to bind in this pocket. The group also revealed that cyclic peptides exhibited pro-apoptotic effects, whereas linear peptides were inactive [20]. Although the binding affinity of the peptides to tubulin was not evaluated in the aforementioned study, it is suspected that the cyclic peptides displayed strong binding affinity to tubulin, resulting in the stabilization of MTs. Hence, the development of cyclic peptides with high affinities toward the Taxol binding pocket is an attractive strategy for the stabilization of MTs.

As a binding motif for the Taxol binding pocket of MTs, we previously described a Tau-derived peptide, **TP** (CGGGKKHVPGGGSVQIVYKPVDL) [21]. **TP** was designed based on a repeat domain in the Tau protein, which is involved in binding to the inner surface of MTs through interactions with the Taxol binding pocket [22, 23]. **TP** binds to the pocket of MTs by preincubation with tubulin and subsequent polymerization of the peptide-tubulin complex [21]. The dissociation constant (K_d) of the tetramethylrhodamine (TMR)-labeled **TP** (**TP-TMR**)-tubulin complex was established as 6.0 μM [21]. We have previously observed the binding of **TP-TMR** to intracellular MTs [24], indicating that **TP** is a suitable binding motif for MTs both in vitro and in living cells. Furthermore, it has been reported that green fluorescent protein (GFP) can be encapsulated inside MTs by conjugation with **TP** [25]. Notably, the GFP-encapsulated MTs exhibited stability similar to the Taxol-bound MTs. Hence, modulation of **TP** for enhancing the binding affinity to the Taxol binding pocket is a promising strategy for stabilizing MTs. In the present study, we successfully developed a TMR-labeled Tau-derived cyclic peptide (**TCP**) for enhanced binding to tubulin and stabilization of MTs (Figure 1).

EXPERIMENTAL

The experimental details, including equipment and materials, estimation of binding affinity by equilibrium dialysis, and CLSM measurement, are available in the Supplementary Information.

Molecular modeling

Molecular mechanics (MM) calculations were performed by a procedure similar to that reported previously using MacroModel 10.4 (Schrödinger, Inc., New York, NY) with optimized potentials for liquid simulations (OPLS) 2005 force field [21]. The refined structure of the tubulin dimer at a resolution of 3.5 Å (PDB ID: 1JFF) [26] was used for the molecular modeling and ligand docking studies. The addition of the missing hydrogen atoms to the model was carried out using Maestro interface ver. 10.4 (Schrödinger) based on an explicit all atom model. The model structures of **TCP1-TMR** and **TCP3-TMR** were constructed based on the structure of **TP** [21], which was based on the reported binding structure of the Tau fragment, Tau(267–312) to MTs (PDB ID: 2MZ7) determined by NMR analysis [23]. The additional residues and the TMR moiety were bound to the NMR structure to prepare **TCP1-TMR** and **TCP3-TMR**, and the energies of the structures were minimized. The obtained **TCP1-TMR** and **TCP3-TMR** structures were placed in the Taxol binding pocket of tubulin instead of Taxol. First, the peptides with the surrounding residues at approximately 5.0 Å were energy-minimized with a shell of constrained residues located within an additional 5.0 Å. The minimum energy conformation was then used as a starting point for a Monte Carlo multiple minimum (MCMM) conformational search analysis to obtain the most favorable conformation and orientation of the peptides. The following parameters were used: up to 1000 search steps, an energy window of 200 kJ/mol for saving structures, and a loosened threshold for conformer redundancy with a root mean square deviation (RMSD) cutoff of 1.0 Å. In the calculations, the peptides with its surrounding residues within 5.0 Å were applied for the

conformational search with a shell of constrained residues located within an additional 4.0 Å. Finally, the obtained structures were energy-minimized by using the same parameters as above. For comparison, minima conformations of **TCP1-TMR** and **TCP3-TMR** in water were searched by a Monte Carlo conformational search with 30000 search steps, an energy window of 100 kJ/mol for saving structures, and a the loosened threshold for conformer redundancy corresponding to a RMSD cutoff of 1.0 Å. From the minima conformations found in the step, the five most stable conformations were superimposed on the binding conformations in the Taxol binding pocket by alignment in the backbone of the core hairpin motif (PGGGSVQIV). The RMSD values of the core hairpin motif between the tubulin-binding conformations and the minima conformations were calculated.

Synthesis of the peptides

For ClAc-C(Acm)-GKKHVPGGGSVQIVYKPVDLC peptide (**TLP1**), H-Cys(Acm)-Gly-Lys(Boc)-Lys(Boc)-His(Trt)-Val-Pro-Gly-Gly-Gly-Ser(Trt)-Val-Gln(Trt)-Ile-Val-Tyr(tBu)-Lys(Boc)-Pro-Val-Asp(OtBu)-Leu-Cys(Trt)-Trt(2-Cl) resin was synthesized on H-Cys(Trt)-Trt(2-Cl)-Resin (Watanabe Chemical Ind. Ltd) using standard Fmoc-based solid-phase chemistry (4 equiv. Fmoc-amino acids). An *N*-methylpyrrolidone (NMP) solution of 1-[(1-(cyano-2-ethoxy-2-oxoethylideneaminooxy)-dimethylamino-morpholinomethylene)] methanaminium hexafluorophosphate (COMU, 4 equiv.) and diisopropylethylamine (DIPEA, 8 equiv.) were used as the coupling reagents. Each condensation was performed at room temperature for 2 h. Deprotection of the Fmoc groups from the resin was performed using 40% and 20% piperidine in *N*,*N*-dimethylformamide (DMF). After the last amino acid coupling, Fmoc deprotection was performed, and the N-terminal amine was chloroacetylated by incubating with 10 equiv. of chloroacetic anhydride in 1 mL of CH_2Cl_2 for 1 h. The peptidyl resin was washed with NMP and

CH_2Cl_2 and then dried under vacuum. The peptide was deprotected (except for the Acm group) and cleaved from the resin by treatment with a cleavage cocktail (trifluoroacetic acid (TFA)/water/thioanisole/ethanedithiol/triisopropylsilane = 86/5/5/3/1, v/v/v/v/v). The mixture was kept at room temperature for 3 h. After filtration, the peptide was precipitated by adding ice-cooled *tert*-butyl methyl ether. After centrifugation, the peptide was washed with *tert*-butyl methyl ether 3 times. The precipitated peptide was dried under vacuum. The crude product was purified by reversed-phase high-performance liquid chromatography (RP-HPLC) with water/acetonitrile (both containing 0.1% TFA, 95/5 to 0/100, v/v for 100 min, linear gradient, 10 mL/min, detected at 220 nm). MALDI-TOF-MS: *m/z* found: 2433 ($[M+H]^+$), calcd. 2433. The ClAc-C(Acm)-GGGKKHVPGGGSVQIVYKPVDLC peptide (**TLP3**) and ClAc-GGGKKHVPGGGSVQIVYKPVDLC peptide (**TLP3c**) were synthesized by the procedure described above. MALDI-TOF-MS for **TLP3**: *m/z* found: 2546 ($[M+H]^+$), calcd. 2547, **TLP3c**: *m/z* found: 2374 ($[M+H]^+$), calcd. 2373.

Cyclization

The cyclization was performed by dissolving **TLP1** or **TLP3** (50 μM) in 0.1 M Tris/HCl, pH 8.1, containing 85 μM dithiothreitol (DTT) and incubating the solution at 25°C for 3 h. In the case of **TLP3c**, **TLP3c** (600 μM) was dissolved in 0.1 M Tris/HCl, pH 8.1, containing 720 μM tris(2-carboxyethyl)phosphine hydrochloride (TCEP-HCl) and incubated at 25°C for 24 h. The resulting cyclic peptides, **TCP1-Cys(Acm)**, **TCP3-Cys(Acm)**, and **TCP3,** were purified by RP-HPLC with water/acetonitrile (both containing 0.1% TFA, 95/5 to 0/100, v/v for 100 min, linear gradient, 10 mL/min, detected at 220 nm). MALDI-TOF-MS for **TCP1-Cys(Acm)**: *m/z* found: 2396 ($[M+H]^+$), calcd. 2397, **TCP3-Cys(Acm)**: *m/z* found: 2510 ($[M+H]^+$), calcd. 2511, **TCP3**: *m/z* found: 2337 ($[M+H]^+$), calcd. 2337.

Labeling of TMR on the cyclic peptides

The S-acetamidomethyl (Acm) groups of **TCP1-Cys(Acm)** and **TCP3-Cys(Acm)** were deprotected by iodine oxidation. HCl (10 equiv.) aqueous solution and iodine (3 equiv.) in methanol were added to **TCP1-Cys(Acm)** or **TCP3-Cys(Acm)** (1.1 mM) in 50% (v/v) acetic acid aqueous solution. The mixture was stirred for 30 min followed by quenching with 1 M ascorbic acid to obtain the target peptides. MALDI-TOF-MS for **TCP1-Cys**: *m/z* found: 2327 ($[M+H]^+$), calcd. 2326, **TCP3-Cys**: *m/z* found: 2440 ($[M+H]^+$), calcd. 2440. The obtained **TCP1-Cys** and **TCP3-Cys** were used for labeling with TMR-5-maleimide without purification. A dimethyl sulfoxide (DMSO) solution of TMR-5-maleimide (100 μM) was added to **TCP1-Cys** and **TCP3-Cys** in 200 mM sodium phosphate buffer, pH 7.0, containing 250 μM TCEP-HCl. The mixture was stirred at 25°C for at least 12 h in the dark. The mixture was dialyzed against water (1 kDa cut-off) and purified by RP-HPLC with water/acetonitrile (both containing 0.1% TFA, 95:5 to 0:100, v/v for 100 min, linear gradient, 10 mL/min, detected at 220 and 551 nm. ESI-QTOF-MS for **TCP3-Cys** analyzed by LC-MS: *m/z* found: 585 ($[M+5H]^{5+}$), calcd. 585, 731 ($[M+4H]^{4+}$), calcd. 731, 974 ($[M+3H]^{3+}$), calcd. 974.

Construction of TCPn-TMR-incorporated GMPCPP MTs

TCP1-TMR or **TCP3-TMR** (375 μM, 1.2 μL) was added to a solution (3.6 μL) containing tubulin (33 μM) and tubulin-AF (33 μM) in BRB80 buffer (80 mM PIPES, pH 6.9, 1.0 mM $MgCl_2$, 1.0 mM EGTA). The mixture (4.8 μL) was kept at 25°C for 30 min in the dark. Then, 1.2 μL of GMPCPP premix (1 mM GMPCPP, 20 mM $MgCl_2$ in BRB80 buffer) was added, and the mixture was kept at 37°C for 30 min in the dark. The mixture was diluted 10-fold with BRB80 buffer and

used for CLSM imaging. For inhibition experiments with Taxol, the mixture was diluted 10-fold with various concentrations of Taxol in BRB80 buffer.

Construction of TCPn-TMR-incorporated GTP MTs

TCP1-TMR, **TCP3-TMR**, **TP-TMR**, or Taxol (100 μM, 2 μL) was added to a solution (6 μL) containing tubulin (3.3 μM) and tubulin-AF (3.3 μM) in BRB80 buffer. The mixture (8 μL) was kept at 25°C for 30 min in the dark. Then, 2 μL of GTP premix (5 mM GTP, 20 mM $MgCl_2$ in BRB80 buffer, 25% (v/v) DMSO) was added, and the mixture was kept at 37°C for 30 min in the dark. **TCP3**-incorporated MTs were prepared by the same procedure using tubulin-TMR instead of tubulin-AF. The mixture was used for CLSM imaging. The length of each MT was determined by using ImageJ software.

Turbidity measurement

Turbidity measurements were performed with tubulin (4 μM) and GTP (1 mM) in the absence or presence of Taxol, **TCP1-TMR**, **TCP3-TMR**, or **TP-TMR** (10 μM) in BRB80 buffer at 37°C. The optical density at 350 nm was monitored with a UV/Vis spectrometer for 60 min at 1 min intervals. After measuring for 60 min, the samples were cooled to 4°C for 15 min, and the optical density was measured again.

RESULTS AND DISCUSSION

To synthesize TMR-labeled **TCP**, a common cyclization method, specifically a coupling reaction between an N-terminal chloroacetyl (ClAc) moiety and the thiol functionality of the C-terminal cysteine residue of the peptide, was utilized to form a thioether bond [27]. **TCP** was designed by introducing a ClAc group on the N-terminus and a cysteine residue on the C-terminus of **TP** to

induce spontaneous cyclization (Figure 2). Furthermore, for labeling with TMR following cyclization, the N-terminal cysteine in the peptide was protected with an S-acetamidomethyl (Acm) group. In addition, different numbers of glycine linkers were introduced to investigate their effects on the binding to MTs. The designed Tau-derived linear peptides, ClAc-C(Acm)-$(G)_n$KKHVPGGGSVQIVYKPVDLC (**TLP1** for n = 1 and **TLP3** for n = 3), were synthesized using standard Fmoc-based solid-phase chemistry and a chloroacetylation reaction of the N-terminal amine of the peptide on the resin. Cyclization of the linear peptides was carried out by incubation in 0.1 M Tris buffer, pH 8.1, at 25°C for 3 h. The resulting cyclic peptides (**TCPn-Cys(Acm)**) were purified by RP-HPLC, and the success of the cyclization was confirmed by MALDI-TOF-MS. The Acm groups of the N-terminal cysteine residues of **TCPn-Cys(Acm)** were subsequently deprotected by iodine oxidation to afford **TCPn-Cys**, as confirmed by MALDI-TOF-MS (Figure 2 and S1) [28]. Finally, the deprotected cysteine residues of **TCPn-Cys** were conjugated with TMR-5-maleimide. The resulting **TCP1-TMR** and **TCP3-TMR** were purified by RP-HPLC, and these compounds were detected by observation of the TMR absorbance at 551 nm. The HPLC retention times of the obtained peptides were different from that of TMR-5-maleimide, confirming the conjugation of TMR to the cyclic peptides (Figure S2). Additionally, LC-MS analysis confirmed the successful formation of **TCP3-TMR** (Figure S3).

The binding of **TCP1-TMR** and **TCP3-TMR** to tubulin was modeled by molecular mechanics (MM) calculations utilizing the MacroModel module. The model structures of **TCP1-TMR** and **TCP3-TMR** were prepared based on the reported binding structure of the Tau fragment, Tau(267–312), to MTs obtained by NMR analysis [23]. The peptides were placed into a Taxol binding pocket of tubulin by replacing the Taxol molecule, and the structures of the peptide-tubulin complexes were energy minimized. Then, a Monte Carlo multiple minimum (MCMM) conformational search was performed to predict the favorable conformations and orientations of

the peptides by randomly varying the torsion angles of the peptides. This method was used to estimate the binding conformations of the cyclic peptides to the target proteins [29, 30]. It was estimated that the core hairpin motifs (PGGGSVQIV) of the peptides fit well into the Taxol binding pocket, and the TMR moieties exhibited no inhibitory effects on the binding of the peptides in the pocket (Figure 3a and 3b). Moreover, the tubulin-binding conformations of **TCP1-TMR** and **TCP3-TMR** were compared with the minima conformations in solution (Figure 3c and 3d). The root mean square deviation (RMSD) values of the core hairpin motif between the tubulin-binding conformations and the minima conformations were within 3.03–3.30 Å for **TCP1-TMR** and 1.70–1.94 Å for **TCP3-TMR**, whereas the RMSD value for **TP** was within 3.45–3.71 Å [21]. Hence, the minimum conformations of the cyclic peptides, in particular **TCP3-TMR**, are expected to be close to the binding conformation in the Taxol binding pocket. The comparison of **TCP1-TMR** and **TCP3-TMR** suggests that **TCP3-TMR**, with a long glycine linker, may adopt a conformation close to the binding conformation in solution. In contrast, **TCP1-TMR**, with a short glycine linker, tends to adopt specific conformations in solution, which may not be as close to the binding conformation as that of **TCP3-TMR**. The conducted MM calculations suggest that the cyclic peptides easily adopt the binding conformation and exhibit enhanced binding to tubulin.

The binding affinities of **TCP1-TMR** and **TCP3-TMR** to tubulin were evaluated by equilibrium dialysis analysis. **TCP1-TMR** and **TCP3-TMR** were incubated with tubulin at various concentrations at 25°C for 1 h. The mixtures were then dialyzed, and the fluorescence intensities of the dialyzed bulk solutions containing the unbound peptides were measured (Figure 4a and 4b). The dissociation constants (K_d values) as well as the binding site occupancies (n values) of **TCP1-TMR** and **TCP3-TMR** per tubulin were estimated by fitting the data using a quadratic binding equation (Figure 4c and 4d). The K_d value of **TCP3-TMR** was estimated to be 0.97 μM, which indicates considerably higher affinity compared to that of linear **TP-TMR** (K_d = 6.0 μM), in which

the N-terminal cysteine residue of **TP** was labeled with TMR (Table 1) [21]. Notably, the affinity of **TCP3-TMR** for tubulin is the highest among the reported peptides that bind to the Taxol binding pocket [17–19]. However, **TCP1-TMR** (K_d = 7.2 μM) displayed a lower affinity than **TP-TMR**. The difference is possibly due to the varying efficiency of the peptides in adopting the binding conformation, as suggested by the MM calculations shown above. The *n* values indicate the binding amount of each peptide per tubulin. Thus, the higher *n* values for **TCP1-TMR** and **TCP3-TMR** compared to that of **TP-TMR** indicate increased numbers of these cyclic peptides bound to tubulin (Table 1).

We subsequently examined the binding of **TCP1-TMR** and **TCP3-TMR** to MTs by confocal laser scanning microscopy (CLSM) (Figure 5). Upon preincubation of the peptides with a mixture of tubulin and green fluorescent Alexa Fluor 430 (AF)-labeled tubulin (tubulin-AF) at 25°C for 30 min, the peptide-tubulin complexes were incubated with guanosine-5'-[(α,β)-methyleno]triphosphate (GMPCPP) at 37°C for 30 min to form MTs (Figure 1b). GMPCPP is a slowly hydrolysable guanosine triphosphate (GTP) analog typically employed in the development of stable MTs [31]. The binding of **TCP1-TMR** and **TCP3-TMR** to the MTs was confirmed by the colocalization of the fluorescence of TMR and AF, which was observed by CLSM (Figure 5b). To verify the binding of the peptides in the Taxol binding pocket of MTs, a competition binding experiment with Taxol was carried out according to a previously reported procedure [21]. The approach was based on the expectation that **TCP1-TMR** and **TCP3-TMR** bound in the Taxol binding pocket would be replaced with Taxol because of the strong binding affinity of Taxol to the pocket (K_d = 10 nM) (Figure 5a) [32]. The TMR fluorescence of **TCP3-TMR** in MTs decreased upon the addition of Taxol, indicating the presence of **TCP3-TMR** in the Taxol binding pocket (Figure 5b). To estimate the amounts of **TCP1-TMR** and **TCP3-TMR** binding to MTs, the TMR and AF fluorescence intensities of each microtubule was calculated from the CLSM images by

ImageJ software. The TMR/AF intensity ratios indicate the amount of peptide binding to the MTs. The TMR/AF ratios of both **TCP1-TMR**- and **TCP3-TMR**-incorporated MTs decreased with increasing Taxol concentration (Figure 5c). Under analogous conditions, most of linear **TP-TMR** was released from the MTs upon exposure to Taxol at a concentration of at least 18 μM [21]. Considering that **TCP1-TMR** and **TCP3-TMR** remained bound to the MTs even at a Taxol concentration of 100 μM (Figure 5c), the binding affinity of the cyclic peptides to the MTs is conceivably higher than that of linear **TP-TMR**.

To evaluate the effects of **TCP1-TMR** and **TCP3-TMR** on the polymerization/depolymerization of MTs, we carried out turbidity measurements. Increases in turbidity are indicative of the formation of MTs. Accordingly, the addition of **TCP3-TMR** to tubulin in the presence of GTP at 37°C increased turbidity, indicating enhanced polymerization of tubulin (Figure 6). This outcome implies that the binding of **TCP3-TMR** in the Taxol binding site promotes tubulin polymerization in a manner similar to that of Taxol [16]. Conversely, **TCP1-TMR** increases the turbidity by a smaller amount than did **TP-TMR**. These variations are a consequence of the different binding affinities of the peptides for tubulin (Table 1). When the temperature was decreased to 4°C to induce depolymerization of the MTs, similar to Taxol-treated MTs, the **TCP1-TMR**- and **TCP3-TMR**-incorporated MTs remained partially stable (Figure 6). On the other hand, the **TP-TMR**-incorporated MTs were completely depolymerized under these conditions. These outcomes demonstrate that, similar to Taxol, the binding of the cyclic peptides, in particular **TCP3-TMR**, increased the stability of MTs by enhancing polymerization and inhibiting depolymerization. The higher stabilization effect of the cyclic peptides compared to the linear peptide is probably due to the strong binding affinity and the increased binding amount of the cyclic peptides to tubulin compared to the linear peptide (Table 1).

The effects of the cyclic peptides on the stability of the MTs were further investigated

by verifying the stability of the MTs prepared with GTP. Typically, GTP-MTs are unstable in vitro due to the hydrolysis of GTP to GDP, leading to the formation of an unstable GDP-tubulin lattice [33], and Taxol is frequently used to stabilize GTP-MTs. Preincubation of the cyclic peptides with a mixture of tubulin and tubulin-AF, followed by incubation with GTP, resulted in the formation of MTs even in the absence of Taxol (Figure 7a and 7b). Notably, **TCP3-TMR** induced the development of long MTs in a manner analogous to that of Taxol (Figure 7c). On the other hand, treatment with **TP-TMR** resulted only in the formation of dot-like structures without MTs (Figure 7d), similar to the case without any treatment (Figure 7e). Hence, **TCP1-TMR** and **TCP3-TMR** were shown to stabilize GTP-MTs, whereas linear **TP-TMR** exhibited no such stabilizing effects. To examine the influence of the TMR moiety in **TCP3-TMR** on the stabilization of MTs, we also synthesized a cyclic **TP** derivative containing three glycine linkers (**TCP3**) that was not labeled with TMR (Figure S4). Analogous to Taxol, **TCP3** also induced the formation of long MTs (Figure S5). This observation suggests that the TMR moiety in **TCP3-TMR** exhibits no apparent effects on the stability of MTs.

In conclusion, in the present study, we effectively synthesized TMR-labeled cyclic Tau-derived peptides to develop new tubulin binding motifs with enhanced affinity to stabilize MTs. We demonstrated that the cyclic peptide **TCP3-TMR** displayed a considerably higher affinity toward tubulin. Moreover, our results confirmed that this analog increased the stability of MTs more significantly than did its linear counterpart (**TP-TMR**). Since the stabilizing effect of **TP-TMR** was not high because of its relatively low binding affinity for tubulin, cyclization is an efficient strategy to improve the binding affinity of the peptides to tubulin for stabilizing MTs. Remarkably, the binding affinity of **TCP3-TMR** is the highest among all peptides previously reported to bind in the Taxol binding pocket of MTs. Since linear **TP-TMR** was shown to penetrate into living cells and bind to intracellular MTs [24], **TCP3-TMR** has potential for applications as

an MT-stabilizing anticancer agent. Moreover, considering that MTs are utilized in various materials applications, including cargo delivery, nanodevices, and molecular robots [34–40], cyclic peptides could be employed for the construction of stable MT-based materials.

ACKNOWLEDGMENTS

We thank Professor Y. Manabe and Professor K. Fukase (Osaka University) for the analysis of the peptides by LC-MS. This work was supported by KAKENHI (No. 17K14517 and 19K15699 for H. I.) from the Japan Society for the Promotion of Science (JSPS), the Inamori Foundation, and Konica Minolta Science and Technology Foundation for Konica Minolta Imaging Science Encouragement Award.

REFERENCES

1. Milroy L-G, Grossmann, TN, Hennig S, Brunsveld L, Ottmann C. Modulators of protein–protein interactions. Chem Rev. 2014;114:4695.
2. Pelay-Gimeno M, Glas A, Koch O, Grossmann, TN. Structure-based design of inhibitors of protein-protein interactions: mimicking peptide binding epitopes. Angew Chem Int Ed. 2015;54:8896.
3. Wójcik P, Berlicki Ł. Peptide-based inhibitors of protein–protein interactions. Bioorg Med Chem Lett. 2016;26:707.
4. Hamley IW. Small bioactive peptides for biomaterials design and therapeutics. Chem Rev. 2017;117:14015.
5. Inaba H, Matsuura K. Peptide nanomaterials designed from natural supramolecular systems. Chem Rec. 2019;19:843.
6. Driggers EM, Hale SP, Lee J, Terrett NK. The exploration of macrocycles for drug discovery – an underexploited structural class. Nat Rev Drug Discov. 2008;7:608.
7. Hill TA, Shepherd NE, Diness F, Fairlie DP. Constraining cyclic peptides to mimic protein structure motifs. Angew Chem Int Ed. 2014;53:13020.
8. Zorzi A, Deyle K, Heinis C. Cyclic peptide therapeutics: past, present and future. Curr Opin Chem Biol. 2017;38:24.
9. Vinogradov AA, Yin Y, Suga H. Macrocyclic peptides as drug candidates: recent progress

and remaining challenges. J Am Chem Soc. 2019;141:4167.

10. Dougherty PG, Sahni A, Pei D. Understanding cell penetration of cyclic peptides. Chem Rev. 2019;119:10241.
11. Udugamasooriya G, Saro D, Spaller MR. Bridged peptide macrocycles as ligands for PDZ domain proteins. Org Lett. 2005;7:1203.
12. Jordan MA, Wilson L. Microtubules as a target for anticancer drugs. Nat Rev Cancer. 2004;4:253.
13. Matamoros AJ, Baas PW. Microtubules in health and degenerative disease of the nervous system. Brain Res Bull. 2016;126:217.
14. Fletcher DA, Mullins RD. Cell mechanics and the cytoskeleton. Nature. 2010;463:485.
15. Hess H, Ross JL. Non-equilibrium assembly of microtubules: from molecules to autonomous chemical robots. Chem Soc Rev. 2017;46:5570.
16. Xiao H, Verdier-Pinard P, Fernandez-Fuentes N, Burd B, Angeletti R, Fiser A, Horwitz SB, Orr GA. Insights into the mechanism of microtubule stabilization by taxol. Proc Natl Acad Sci USA. 2006;103:10166.
17. Biswas A, Kurkute P, Saleem S, Jana B, Mohapatra S, Mondal P, Adak A, Ghosh S, Saha A, Bhunia D, Biswas SC, Ghosh S. Novel hexapeptide interacts with tubulin and microtubules, inhibits Aβ fibrillation, and shows significant neuroprotection. ACS Chem Neurosci. 2015;6:1309.
18. Mondal P, Das G, Khan J, Pradhan K, Ghosh S. Crafting of neuroprotective octapeptide from taxol-binding pocket of β-tubulin. ACS Chem Neurosci. 2018;9:615.
19. Mondal P, Das G, Khan J, Pradhan K, Mallesh R, Saha A, Jana B, Ghosh S. Potential neuroprotective peptide emerged from dual neurotherapeutic targets: a fusion approach for the development of anti-alzheimer's lead. ACS Chem Neurosci. 2019;10:2609.
20. Brindisi M, Maramai S, Brogi S, Fanigliulo E, Butini S, Guarino E, Casagni A, Lamponi S, Bonechi C, Nathwani SM, Finetti F, Ragonese F, Arcidiacono P, Campiglia P, Valenti S, Novellino E, Spaccapelo R, Morbidelli L, Zisterer DM, Williams CD, Donati A, Baldari C, Campiani G, Ulivieri C, Gemma S. Development of novel cyclic peptides as pro-apoptotic agents. Eur J Med Chem. 2016;117:301.
21. Inaba H, Yamamoto T, Kabir AMR, Kakugo A, Sada K, Matsuura K. Molecular encapsulation inside microtubules based on Tau-derived peptides. Chem Eur J. 2018;24:14958.
22. Kar S, Fan J, Smith MJ, Goedert M, Amos LA. Repeat motifs of tau bind to the insides of microtubules in the absence of taxol. EMBO J. 2003;22:70.
23. Kadavath H, Jaremko M, Jaremko Ł, Biernat J, Mandelkow E, Zweckstetter M. Folding of the Tau protein on microtubules. Angew Chem Int Ed. 2015;54:10347.

24. Inaba H, Yamamoto T, Iwasaki T, Kabir AMR, Kakugo A, Sada K, Matsuura K. Fluorescent Tau-derived peptide for monitoring microtubules in living cells. ACS Omega. 2019;4:11245.
25. Inaba H, Yamamoto T, Iwasaki T, Kabir AMR, Kakugo A, Sada K, Matsuura K. Stabilization of microtubules by encapsulation of the GFP using a Tau-derived peptide. Chem Commun. 2019;55:9072.
26. Löwe J, Li H, Downing KH, Nogales E. Refined structure of αβ-tubulin at 3.5 Å resolution. J Mol Biol. 2001;313:1045.
27. Hipolito CJ, Suga H. Ribosomal production and in vitro selection of natural product-like peptidomimetics: the FIT and RaPID systems. Curr Opin Chem Biol. 2012;16:196.
28. Kamber B, Hartmann A, Eisler K, Riniker B, Rink H, Sieber P, Rittel W. The synthesis of cystine peptides by iodine oxidation of S-trityl-cysteine and S-acetamidomethyl-cysteine peptides. Helv Chim Acta. 1980;63:899.
29. Jiang S, Liao C, Bindu L, Yin B, Worthy KW, Fisher RJ, Burke TR, Nicklaus MC, Roller PP. Discovery of thioether-bridged cyclic pentapeptides binding to Grb2-SH2 domain with high affinity. Bioorg Med Chem Lett. 2009;19:2693.
30. Roxin Á, Chen J, Scully CCG, Rotestein BH, Yudin AK, Zheng G. Conformational modulation of in vitro activity of cyclic RGD peptides via aziridine aldehyde-driven macrocyclization chemistry. Bioconjugate Chem. 2012;23:1387.
31. Hyman AA, Salser S, Drechsel DN, Unwin N, Mitchison TJ. Role of GTP hydrolysis in microtubule dynamics: information from a slowly hydrolyzable analogue, GMPCPP. Mol Biol Cell. 1992;3:1155.
32. Caplow M, Shanks J, Ruhlen R. How taxol modulates microtubule disassembly. J Biol Chem. 1994;269:23399.
33. Alushin GM, Lander GC, Kellogg EH, Zhang R, Baker D, Nogales E. High-resolution microtubule structures reveal the structural transitions in αβ-tubulin upon GTP hydrolysis. Cell. 2014;157:1117.
34. Hess H, Vogel V. Molecular shuttles based on motor proteins: active transport in synthetic environments. Rev Mol Biotechnol. 2001;82:67.
35. Kabir AMR, Kakugo A. Study of active self-assembly using biomolecular motors. Polym J. 2018;50:1139.
36. Bachand GD, Spoerke ED, Stevens MJ. Microtubule-based nanomaterials: exploiting nature's dynamic biopolymers. Biotechnol Bioeng 2015;112:1065.
37. Sato Y, Hiratsuka Y, Kawamata I, Murata S, Nomura S-IM. Micrometer-sized molecular robot changes its shape in response to signal molecules. Sci Rob. 2017;2:eaal3735.
38. Keya JJ, Suzuki R, Kabir AMR, Inoue D, Asanuma H, Sada K, Hess H, Kuzuya A, Kakugo A. DNA-assisted swarm control in a biomolecular motor system. Nat Commun. 2018;9:453.

39. Matsuda K, Kabir AMR, Akamatsu N, Saito A, Ishikawa S, Matsuyama T, Ditzer O, Islam MS, Ohya Y, Sada K, Konagaya A, Kuzuya A, Kakugo A. Artificial smooth muscle model composed of hierarchically ordered microtubule asters mediated by DNA origami nanostructures. Nano Lett. 2019;19:3933.
40. Inoue D, Gutmann G, Nitta T, Kabir AMR, Konagaya A, Tokuraku K, Sada K, Hess H, Kakugo A. Adaptation of patterns of motile filaments under dynamic boundary conditions. ACS Nano. 2019;13:12452.

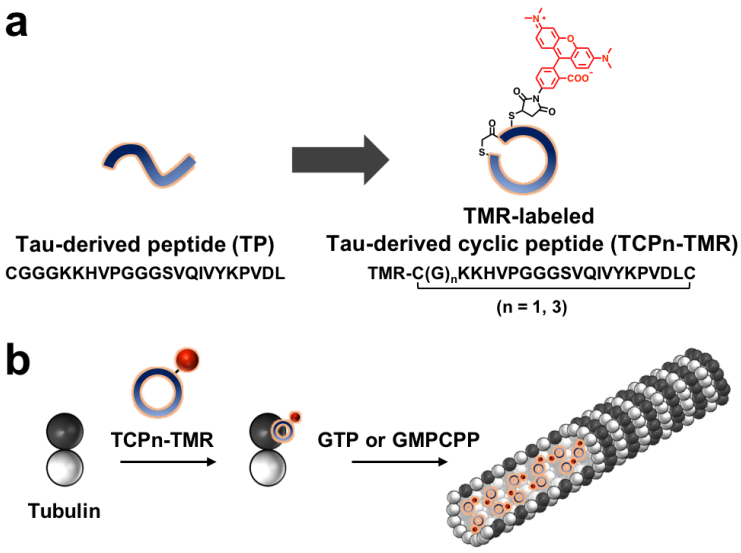

Figure 1. (a) Tetramethylrhodamine (TMR)-labeled Tau-derived cyclic peptide (**TCPn-TMR**) (n= 1, 3) designed from the Tau-derived peptide (**TP**), a binding motif for microtubules (MTs) [21]. (b) Binding of **TCPn-TMR** inside MTs by preincubation with tubulin and subsequent polymerization.

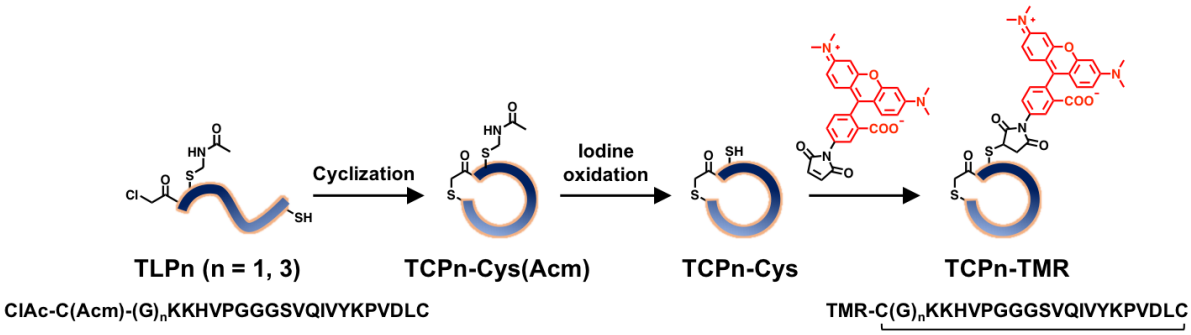

Figure 2. Synthesis of **TCPn-TMR** from **TLPn** (n = 1, 3).

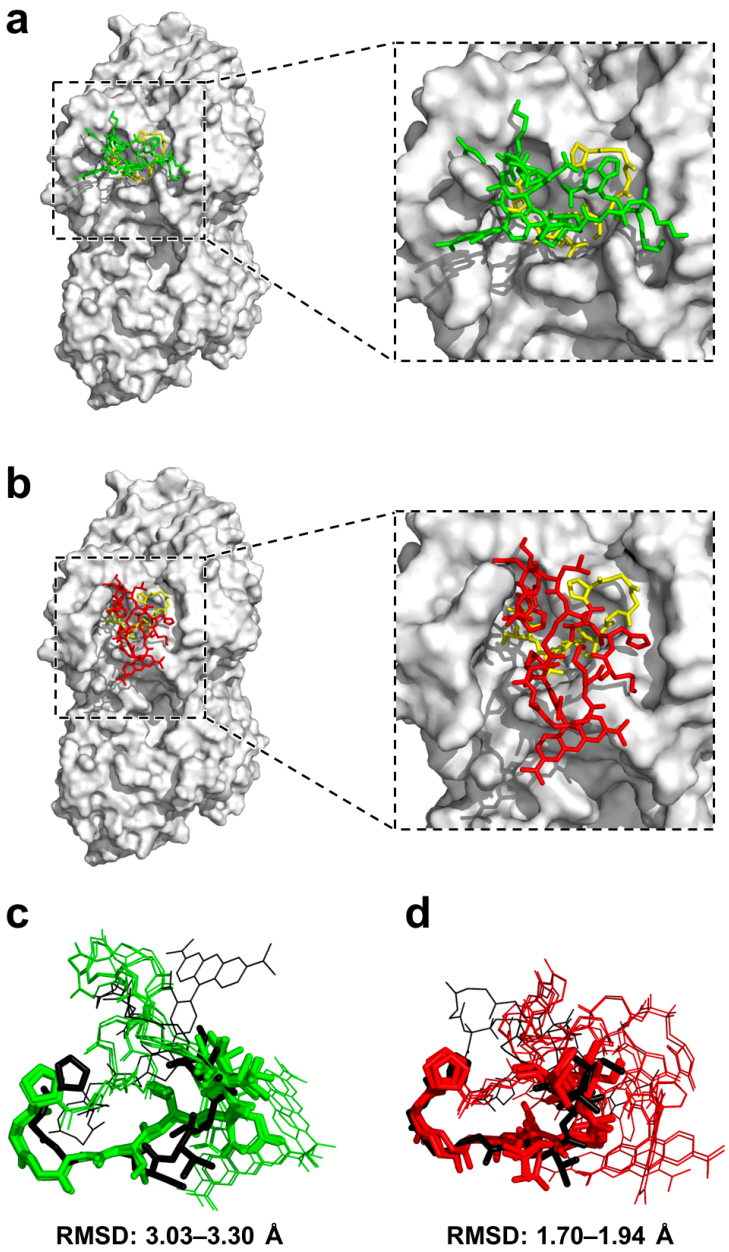

Figure 3. Model of the binding of (a) **TCP1-TMR** and (b) **TCP3-TMR** (stick representation) in the Taxol binding pocket of tubulin obtained by molecular mechanics (MM) calculations. Yellow indicates the core hairpin motif (PGGGSVQIV). The backbone conformations of (c) **TCP1-TMR** and (d) **TCP3-TMR** aligned in the core hairpin motif (stick representations). The binding conformations in the Taxol binding pocket are shown in black. The minimum conformations from the global minima are indicated in green (**TCP1-TMR**) and red (**TCP3-TMR**).

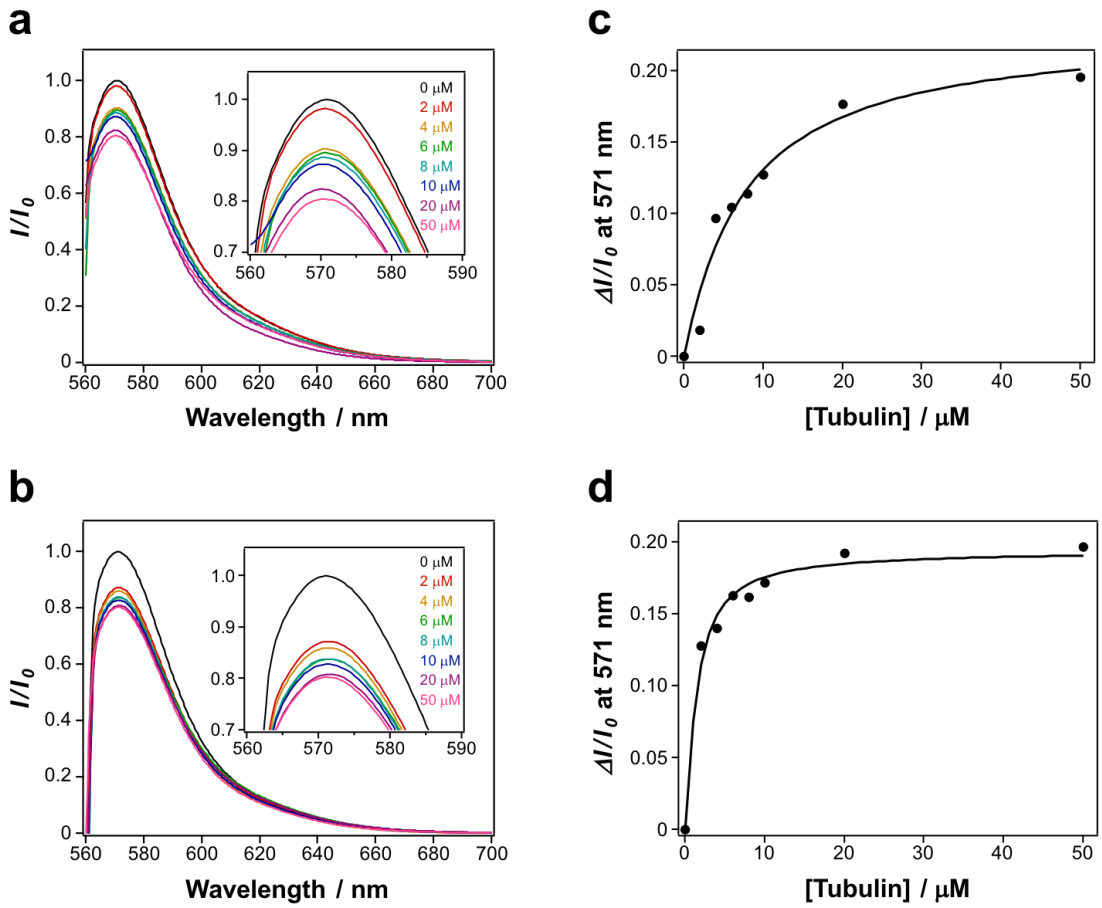

Figure 4. Estimation of the binding affinity of **TCPn-TMR** for tubulin by equilibrium dialysis. Fluorescence spectra of the dialyzed bulk solution following dialysis of 1 μM (a) **TCP1-TMR** and (b) **TCP3-TMR** in the presence of 0–50 μM tubulin. The binding parameters of (c) **TCP1-TMR** and (d) **TCP3-TMR** to tubulin analyzed from (a) and (b), respectively. Closed circles show experimental values, while the solid lines are theoretical curves obtained by fitting the dissociation constant (K_d) and the binding site occupancy ($n = \Delta I_{max}/I_0$) at 571 nm.

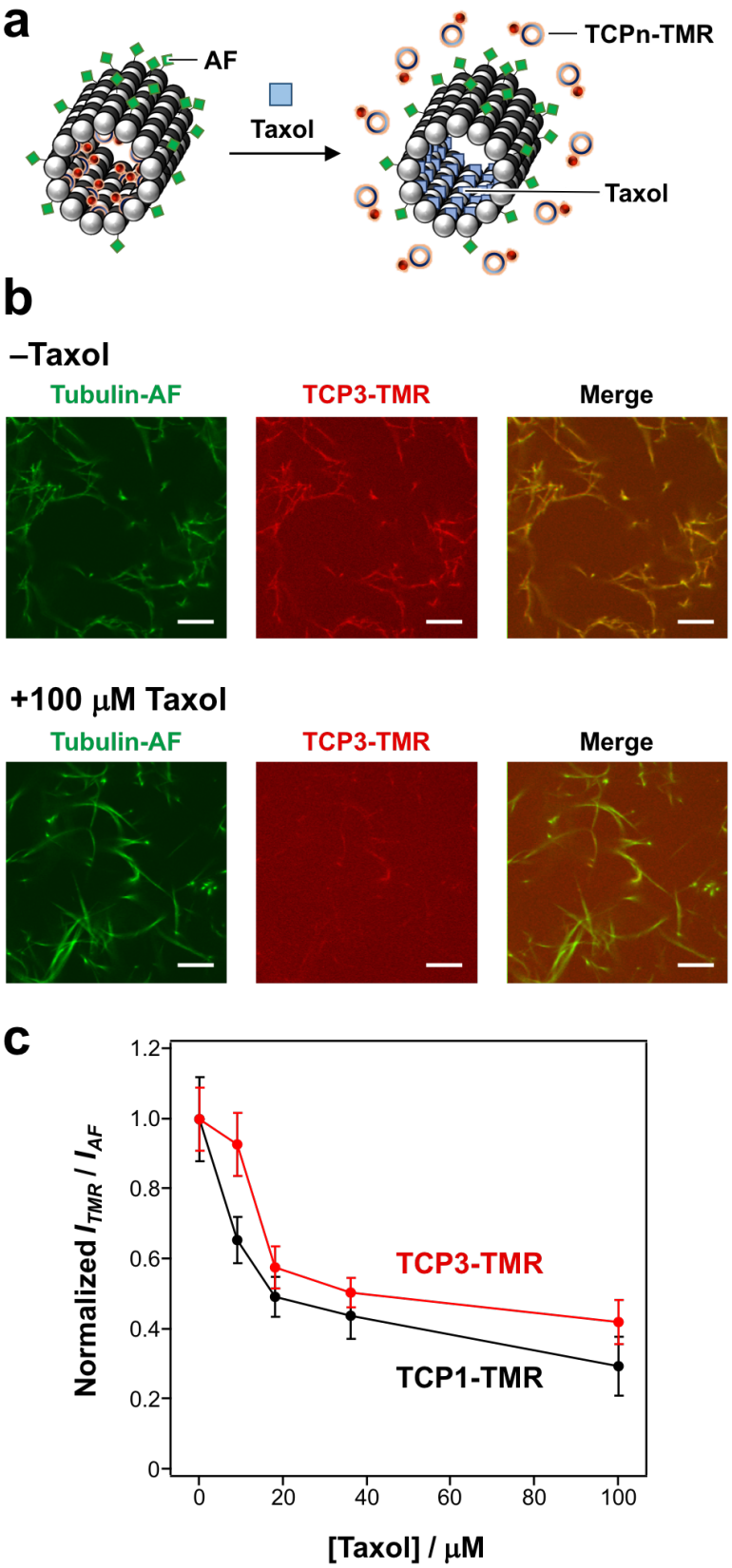

Figure 5. (a) Substitution of **TCPn-TMR** in MTs by Taxol. (b) Confocal laser scanning microscopy (CLSM) images of Alexa Fluor 430 (AF)-labeled GMPCPP MTs prepared with **TCP3-TMR** and further treatment in the presence and absence of 100 μM Taxol (scale bar: 10 μm). Final concentrations: [Tubulin] = [Tubulin-AF] = 2 μM, [**TCP3-TMR**] = 7.5 μM, [Taxol] = 100 μM,

[GMPCPP] = 20 μM. (c) Effect of the concentration of Taxol on the TMR fluorescence (I_{TMR}) per AF fluorescence (I_{AF}) of **TCP1-TMR**- and **TCP3-TMR**-incorporated MT. I_{TMR}/I_{AF} was normalized using the value obtained without Taxol. The error bars represent the SEM (N =20).

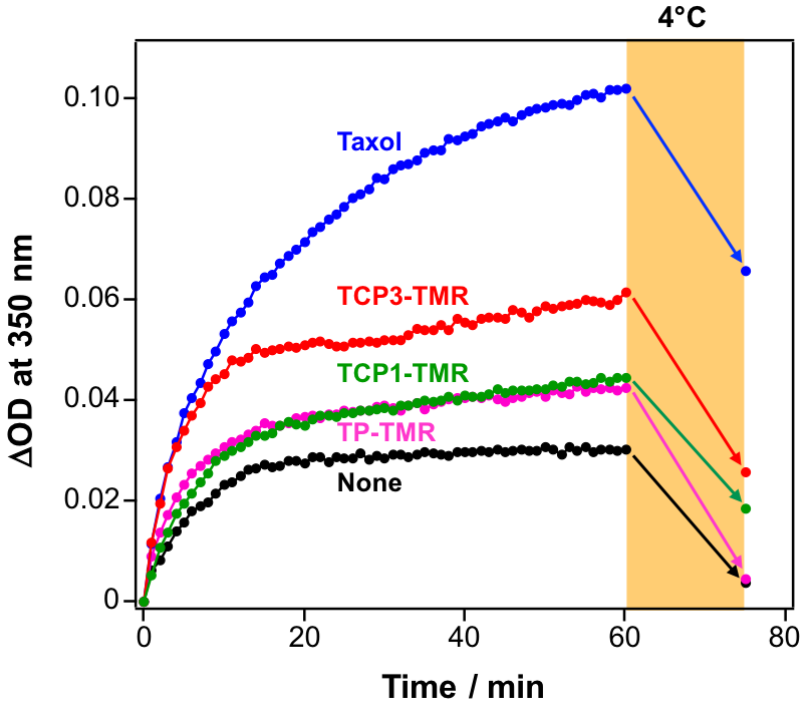

Figure 6. Changes in turbidity over time as a result of tubulin polymerization. The optical density at 350 nm was measured with 4 μM tubulin and 1 mM GTP in the absence (black) or presence of 10 μM Taxol (blue), **TCP1-TMR** (green), **TCP3-TMR** (red), or **TP-TMR** (magenta) at 37°C. After measurement for 60 min, the samples were cooled to 4°C for 15 min and measured again.

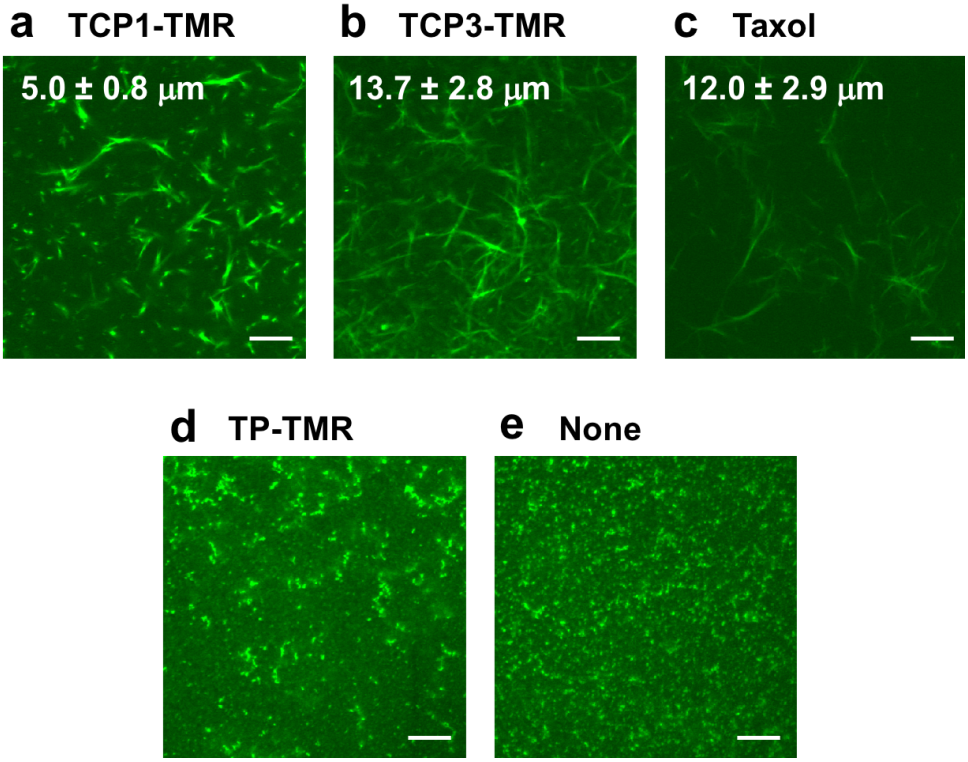

Figure 7. CLSM images of AF-labeled GTP-MTs preincubated with (a) **TCP1-TMR**, (b) **TCP3-TMR**, (c) Taxol, (d) **TP-TMR**, and (e) without any additive (scale bar: 10 μm). Final concentrations: [Tubulin] = [Tubulin-AF] = 4 μM, [**TCP1-TMR**] = [**TCP3-TMR**] = [Taxol] = [**TP-TMR**] = 20 μM, [GTP] = 1 mM. The lengths of MTs (average ± standard deviation) are shown.

Table 1. Binding affinity of the TMR peptides to tubulin.

Sample	K_d (μM)	Binding site occupancy (n)
TCP1-TMR	7.2	0.23
TCP3-TMR	0.97	0.19
TP-TMR [21]	6.0	0.12